

UV-Driven Evolution and Chemistry of Protoplanetary Disks: Insights from *HST*'s ULLYSES Program



STScI | SPACE TELESCOPE SCIENCE INSTITUTE

Nicole Arulanantham*
Giacconi Fellow, STScI
narulanantham@stsci.edu



Motivation

Accreting T Tauri stars generate strong UV radiation fields, which regulate gas-phase chemistry in protoplanetary disks and establish the inventories of volatile-bearing molecules. However, there has previously been little overlap between the population of disks with available UV spectroscopy and those with sub-mm and/or infrared observations of molecular gas, limiting statistical studies of how UV radiation fields impact the physical and chemical structure of disks while accretion is ongoing.

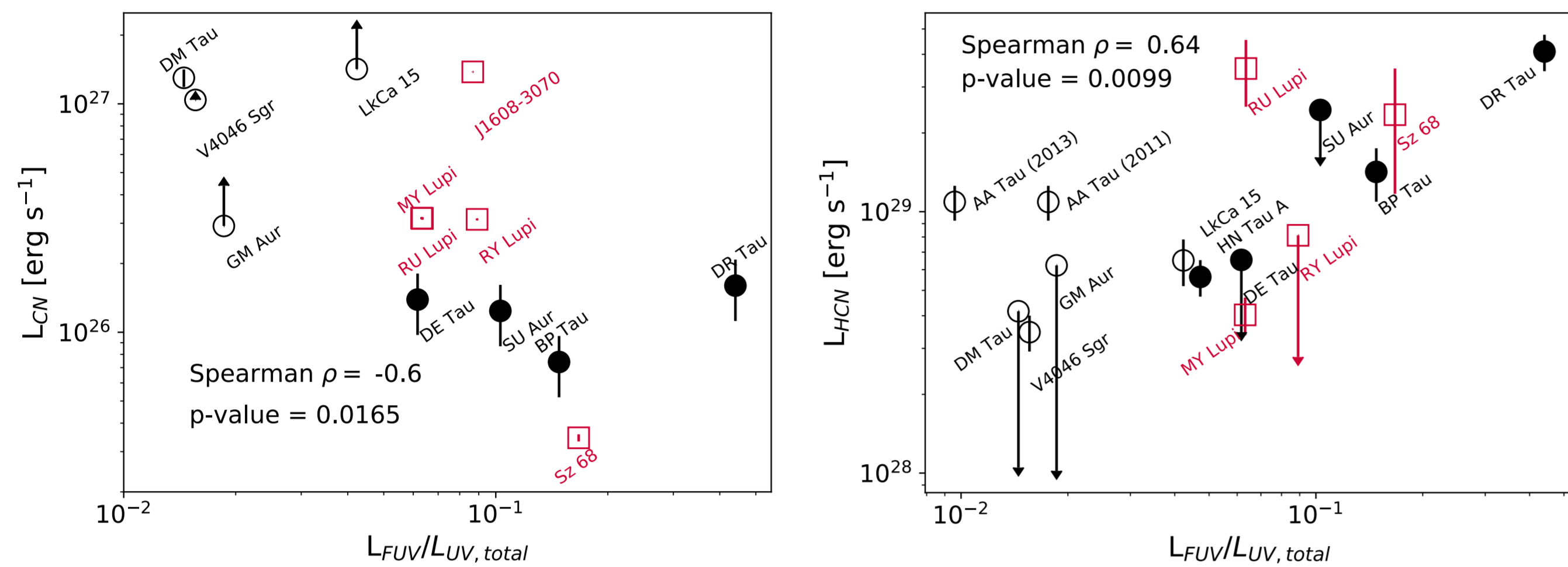
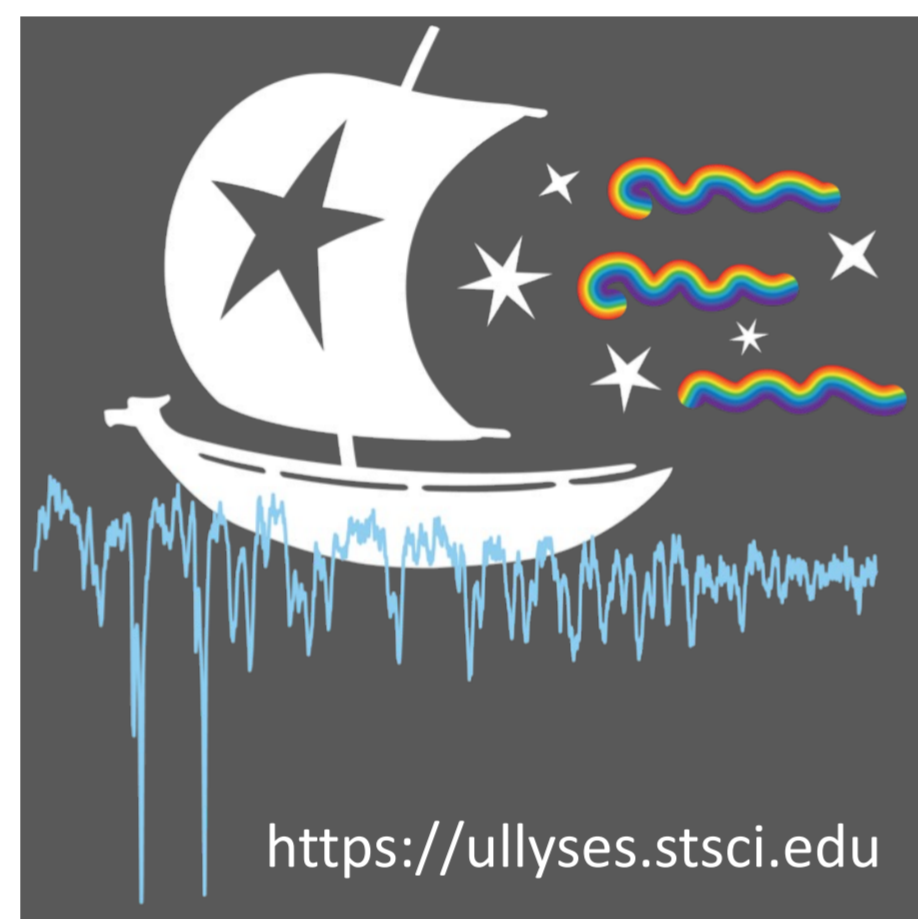


Fig. 1: At face value, targets with stronger FUV radiation fields show weaker sub-mm CN emission (left) and stronger IR HCN (right). However, the small sample size makes it difficult to observationally isolate the impact of UV irradiation on the underlying abundances from other factors (e.g., C/O, disk temperature structure; Arulanantham+ 2020).

Targets and Observations

The sample of T Tauri stars with uniform UV spectroscopy from *HST* recently expanded to $N = 112$, through the Ultraviolet Legacy Library of Young Stars as Essential Standards (ULLYSES) Director's Discretionary program (Roman-Duval+ 2020). The spectra include Ly α emission, which contributes $\sim 88\%$ of the total UV flux (France+ 2014), on average, after undergoing millions of scattering events within the protostellar environment. This allows the radiation to penetrate deeper into the gas layer than continuum photons (see e.g., Bergin+ 2003, Bethell & Bergin 2011). Fluorescent H $_2$ emission lines are also detected, from molecules that are pumped into excited electronic transitions by Ly α photons (see e.g., Herczeg+ 2002, France+ 2012, Hoadley+ 2015).



Results: Linking Ly α Emission to Protoplanetary Disk Observations

We find that the shapes of the Ly α emission lines from T Tauri stars, parametrized by the ratios of red ($\lambda > 1215.67$ Angstroms) to blue ($\lambda < 1215.67$ Angstroms) flux, are correlated with the infrared spectral indices and occurrence rates of high-velocity forbidden emission line components (Arulanantham+ 2021). We also find that the H I velocities derived from simple shell scattering models are statistically significantly correlated with the shapes of the Ly α profiles and K-band veiling, indicating that the turnover in Ly α profile shape occurs as excess emission from $T = 2000$ K dust disappears, although the dust clearing mechanisms are difficult to constrain without high-resolution images of the infrared and sub-mm continuum (Arulanantham+ 2023). Together these results imply that the UV radiation fields and protoplanetary disks evolve in unison throughout the process of planet formation.

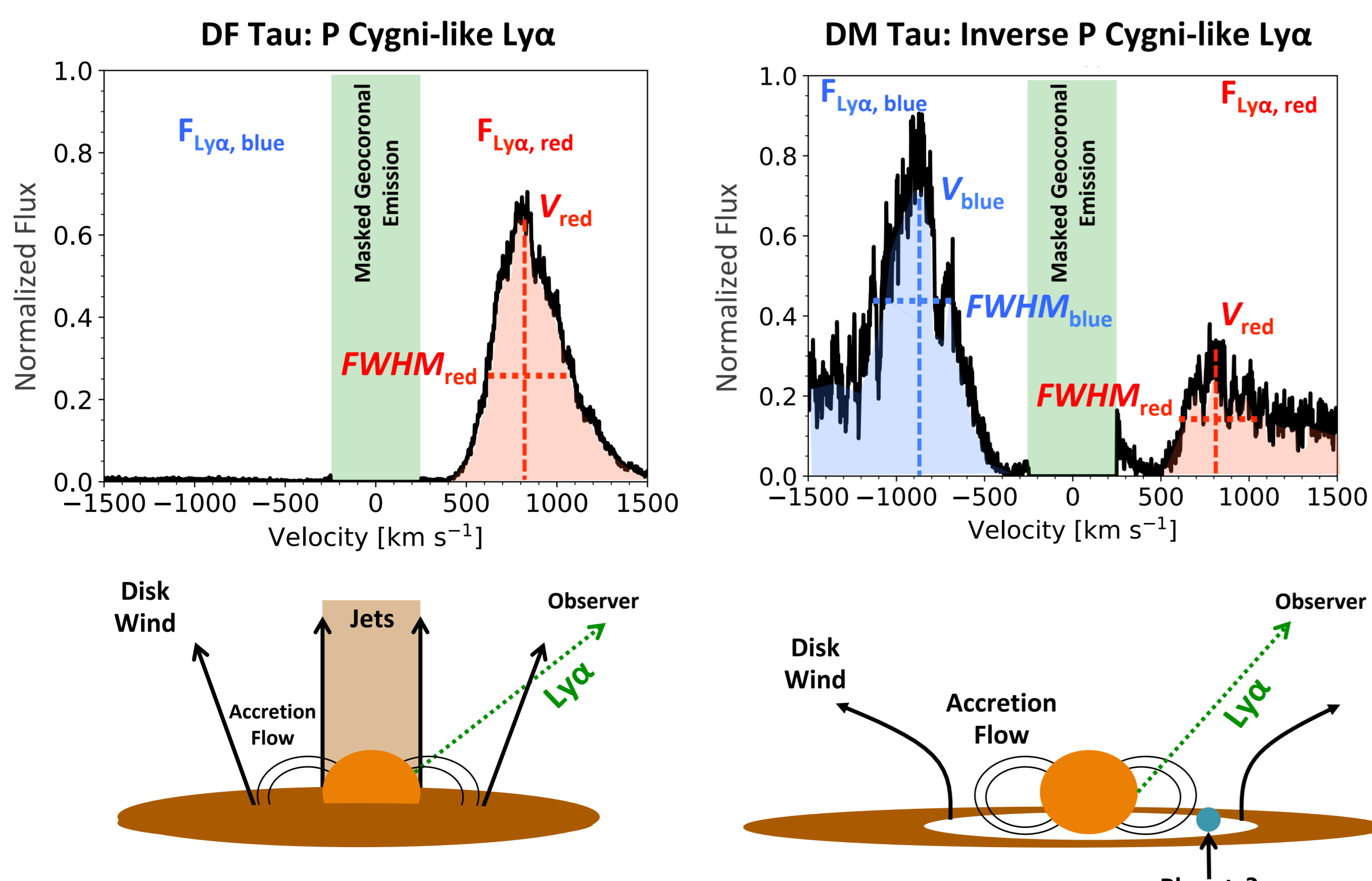


Fig. 2: Illustration of characteristic Ly α emission line shapes and corresponding stages of protoplanetary disk evolution (Arulanantham+ 2023). The turnover from P Cygni-like to inverse P Cygni-like Ly α profile indicates that there is significant evolution in UV irradiation of molecular gas over the disk lifetimes.

Results: Constraining Disk Vertical Structure

The dominant formation pathway for CN molecules in protoplanetary disks requires a population of vibrationally excited H $_2$ (H $_2^*$), at temperatures consistent with surface layers of the disks ($T = 2000$ K; Visser+ 2018, Cazzoletti+ 2018). The population of H $_2^*$ at $r < 10$ au can absorb Ly α photons, producing fluorescent emission lines observed in the ULLYSES spectra from *HST* (France+ in prep). We use a grid of DALI models (Bruderer+ 2012) to explore whether the UV-fluorescent H $_2$ emission lines can help untangle degeneracies between disk flaring, UV irradiation, and disk mass. The distributions of H $_2^*$ from the models are input to a Ly α radiative transfer code (Hoadley+ 2015) to fit the observed UV spectra from RY Lup and MY Lup (Arulanantham+, in prep).

	RY Lup	MY Lup
UV Luminosity	4.94e30 erg/s	3.5e29 erg/s
CN Luminosity	2.2e25 erg/s	2.3e25 erg/s
References	Langlois+ 2018, Arulanantham+ 2018, van Terwisga+ 2019	Avenhaus+ 2018, Arulanantham+ 2020, van Terwisga+ 2019

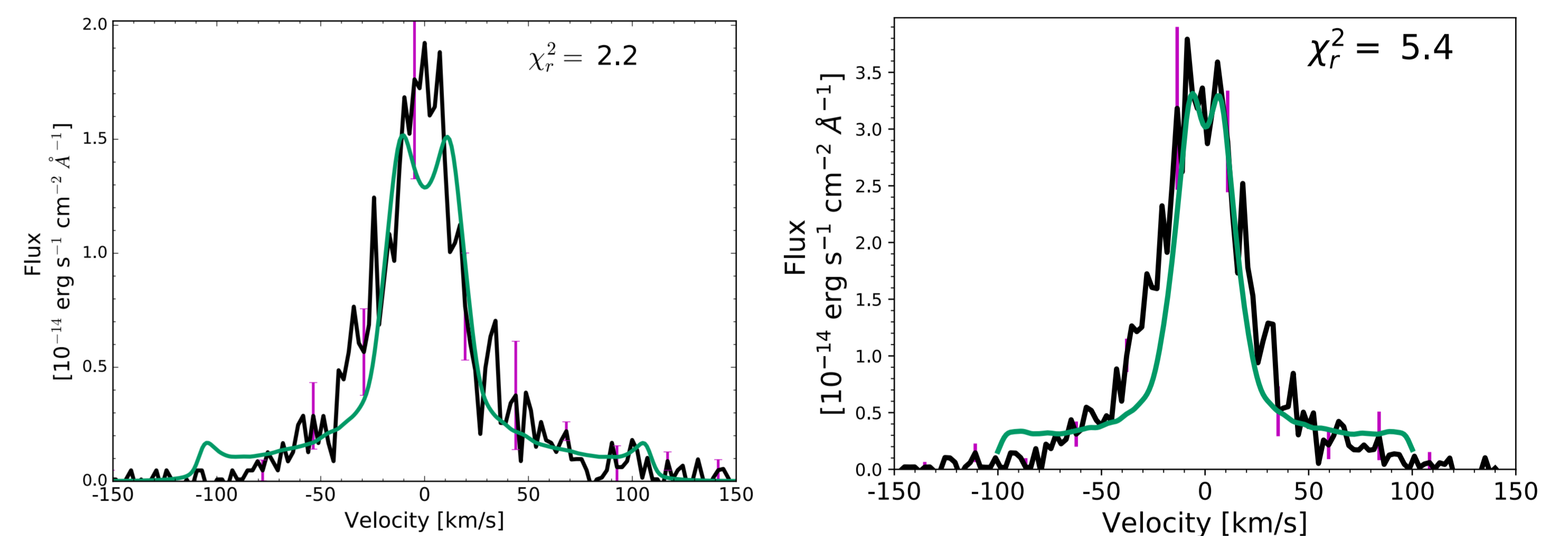


Fig. 3: UV-fluorescent H $_2$ emission (black) and best-fit DALI models (green) for MY Lup (left) and RY Lup (right; Arulanantham+ in prep). The spectrum from MY Lup is well fit by a flared disk model with large gas mass ($0.1 M_{\odot}$) and low UV luminosity ($0.015 L_{\odot}$). The spectrum from RY Lup is also well fit by a flared disk model but requires a lower gas mass ($0.001 M_{\odot}$) and higher UV luminosity ($0.15 L_{\odot}$), consistent with observations of both systems. A two sample Welch's t -test confirms that the two datasets cannot be reproduced by the same model ($t = 6.9$; $p = 10^{-10}$).

Conclusions: Implications for Physical-Chemical Disk Models

Multi-wavelength synergies are now possible with UV spectra from ULLYSES and IR and sub-mm observations of molecular gas. **Together, these datasets may be used to more accurately construct physical-chemical models of protoplanetary disks, providing updated chemical inventories for models of planet formation.** We do not find a statistically significant relationship between total observed Ly α flux and stellar mass in this sample of K and M-type YSOs, indicating that the expected relationship between disk temperature structure and host star spectral type is more complex than a linear trend and perhaps reflects the scatter in the relationship between stellar mass and accretion rate (see e.g., PPVII Chapter 15). Some of these degeneracies may be untangled by using UV-fluorescent H $_2$ emission lines to anchor models of UV-sensitive molecules like CN, HCN, and C $_2$ H.

Future Work & Acknowledgements

We are reconstructing the Ly α emission reaching warm molecular gas in the inner disks of ULLYSES targets, to explore how photodissociation rates might change over the disk lifetimes (Arulanantham, Ortiz-Quintana+ in prep)

We are also exploring Ly α propagation through the disk winds, which may enhance UV irradiation of gas at large radii (Chang, Arulanantham+, in prep). This modeling framework is presented in Chang+ 2022, where it was developed for studies of AGN and star-forming galaxies.

**These projects were done in collaboration with Max Gronke, Eleonora Fiorellino, Jorge Filipe Gameiro, Antonio Frasca, Joel Green, Sierk van Terwisga, Anna Miotello, and the ODYSSEUS and PENELLOPE teams. Based on observations obtained with the NASA/ESA Hubble Space Telescope, retrieved from the Mikulski Archive for Space Telescopes (MAST) at the Space Telescope Science Institute (STScI). STScI is operated by the Association of Universities for Research in Astronomy, Inc. under NASA contract NAS 5-26555.*

References

- Arulanantham, N., France, K., Hoadley, K., et al. 2018, *ApJ*, 855:2
 Arulanantham, N., France, K., Cazzoletti, P., et al. 2020, *AJ*, 159:4
 Arulanantham, N., France, K., Hoadley, K., et al. 2021, *AJ*, 162:5
 Arulanantham, N., Gronke, M., Fiorellino, E., et al. 2023, *ApJ*, 944:2
 Avenhaus, H., Quanz, S.P., Garufi, A., et al. 2018, *ApJ*, 863:1
 Bergin, E., Calvet, N., D'Alessio, P., & Herczeg, G.J. 2003, *ApJ*, 591:2
 Bethell, T.J. & Bergin, E.A. 2011, *ApJ*, 739:2
 Bruderer, S., van Dishoeck, E.F., Doty, S.D., & Herczeg, G.J. 2012, *A&A*, 541, A91
 Cazzoletti, P., van Dishoeck, E.F., Visser, R., et al. 2018, *A&A*, 609, A93
 Chang, S.-J., Yang, Y., Seon, K.-I., et al. 2023, *ApJ*, 945:2
 France, K., Schindhelm, R., Herczeg, G.J., et al. 2012, *ApJ*, 756:2
 France, K., Schindhelm, R., Bergin, E.A., et al. 2014, *ApJ*, 784:2
 Herczeg, G.J., Linsky, J.L., Valenti, J.A., et al. 2002, *ApJ*, 572:1
 Hoadley, K., France, K., Alexander, R.D., et al. 2015, *ApJ*, 812:1
 Langlois, M., Pohl, A., Lagrange, A.-M., et al. 2018, *A&A*, 614, A88
 Van Terwisga, S.E., van Dishoeck, E.F., Cazzoletti, P. et al. 2019, *A&A*, 623, A150
 Visser, R., Bruderer, S., Cazzoletti, P., et al. 2018, *A&A*, 615, A75
 Roman-Duval, J., Proffitt, C.R., Taylor, J.M., et al. 2020, *RNAAS*, 4:11